

## Structure and properties of anisotropic gels and plasticized networks containing molecules with a smectic-*A* phase

R. A. M. Hikmet and R. Howard

*Philips Research, Prof. Holstlaan 4, 5656AA Eindhoven, The Netherlands*

(Received 25 February 1993)

Liquid-crystal (LC) mixtures of a low-molar-mass LC diacrylate and 4-cyano-4'-octylbiphenyl (8CB) showing a smectic-*A* phase in the bulk were produced. The mixtures were aligned macroscopically and the polymerization was induced photochemically. In this way, anisotropic networks containing molecules which are not chemically attached to the network (anisotropic gels and plasticized networks) were produced. Using IR dichroism, it was found that, above the nematic-to-isotropic transition temperature of 8CB, a fraction of the molecules remained oriented. This behavior was associated with the presence of two populations of 8CB molecules within anisotropic gels and plasticized networks. One of the populations showed the same behavior as in the bulk (unbound fraction), while the other population was found to be influenced to a large extent by the network (bound fraction) and did not show a first-order nematic-to-isotropic transition. The behavior as observed by IR dichroism was simulated using a theoretical model and the fractions of the bound and unbound 8CB were estimated in systems containing various amounts of networks.

PACS number(s): 64.70.Md, 82.70.-y, 61.30.-v

### INTRODUCTION

In the past few years reports describing the properties and applications of anisotropic gels and plasticized networks have appeared [1–5]. These materials are obtained by producing a liquid-crystal (LC) mixture containing conventional low-mass LC molecules and LC molecules with polymerizable groups. Long-range orientation of the mixture is induced at specially treated interfaces, in an electric or magnetic field. By photochemically induced polymerization of the mixture, anisotropic gels and plasticized networks are produced. These systems consist of interconnected phases of a three-dimensional anisotropic network and molecules (free molecules) which are not chemically attached to the network. These systems are of great interest since they provide new challenges concerning the behavior of LC molecules in anisotropic confinements [1–3] as well as showing optical effects to be used in display applications [4,5].

In our previous publications [1,2] describing anisotropic gels and plasticized networks, it was shown that the fraction of the free molecules showing the first-order nematic-to-isotropic phase transition decreased with increasing network concentration. In the case of systems with very high concentrations of network the transition was totally absent. Using dielectric spectroscopy [2], this behavior was associated with the presence of a distribution of domain sizes within the system, with a critical domain size below which the first-order nematic-to-isotropic transition becomes suppressed. In a recent work concerning cholesteric gels [3], relying on the selective optical reflectivity of the system the critical domain size was estimated to be on the order of 85 nm. Furthermore, it was deduced that in these cholesteric gels the free molecules are confined between layers of the net-

work. This deduction was further supported by a more recent work [6], where it was shown that the removal of the free molecules from the gels by evaporation resulted in a uniaxial collapse of the cholesteric helix without further change in the optical quality of the gels. In the study presented here, we used 4-cyano-4'-octylbiphenyl (8CB) with a smectic-*A* phase as free molecules within the anisotropic gels and plasticized networks in order to study the structure of the systems and the behavior of the free molecules within them. IR dichroism was used to elaborate on the previously suggested two-phase model in order to explain the behavior of the two populations of the free molecules. The changes occurring during polymerization were followed by monitoring the optical retardation through the samples as a function of time. Furthermore, x-ray diffraction in combination with scanning electron microscopy was used to estimate the structure of the systems.

### EXPERIMENT

The LC diacrylate 1,4-di-(4-(6-acryloyloxyhexyloxy)benzoyloxy)-2-methylbenzene (C6M) used in this study was synthesized within our laboratory and its properties have been described in previous publications [5,7] and 8CB is a commercial product purchased from Merck (Poole). In order to initiate polymerization, LC mixtures were provided with 0.5% w/w Irgacure 651 (Ciba Geigy). Transition temperatures and the polymerization of the mixtures were followed using a Perkin-Elmer Model DSC-2C differential scanning calorimeter provided with an UV source ( $0.2 \text{ mW cm}^{-2}$ ). In the experiments, sample quantities of 5 mg were used and the atmosphere in the DSC was chosen to be nitrogen. Optical properties of the materials were studied using a polarizing microscope

provided with a rotary compensator, photomultiplier, and a Mettler heating stage. For the optical measurements cells with a gap of  $6\ \mu\text{m}$  provided with uniaxially rubbed polymer layers were filled with the LC mixture in order to obtain uniaxially aligned samples. Infrared measurements were carried out using a Bruker Model IFS45 Fourier-transform IR (FTIR) spectrometer equipped with a wire grid polarizer. Uniaxially oriented samples for IR measurements were obtained between KBr plates provided with uniaxially rubbed nylon layers. For x-ray-diffraction measurements a Statton camera and Ni-filtered  $\text{Cu } K\alpha$  radiation were used. The samples used for the x-ray measurements were prepared in cells with a gap of  $60\ \mu\text{m}$  where the molecular alignment was induced under an electric field.

### RESULTS AND DISCUSSION

The mesomorphic behavior of the pure components and their mixtures containing the initiator was studied by DSC and optical microscopy. The nematic-to-isotropic transition temperature ( $T_c$ ) for the mixtures increased almost linearly from  $40\ ^\circ\text{C}$  (for pure 8CB) to  $116\ ^\circ\text{C}$  (for pure C6M) with increasing weight fraction of C6M. The smectic-*A* phase shown by pure 8CB at around  $33\ ^\circ\text{C}$  could also be observed in mixtures containing up to 10% w/w C6M. Mixtures of various compositions were polymerized at various temperatures to produce anisotropic gels and plasticized networks. The behavior of C6M and 8CB molecules after polymerization was studied using DSC and IR. In Fig. 1, DSC curves for various polymerized samples (gels) are shown. It can be seen that the onset of the nematic-to-isotropic transition remains the same with increasing network concentration, while the peaks become broader. The significance of this first-order transition within the system will become clearer later in the text. For systems containing higher concentrations (30% w/w) of polymerized C6M (anisotropic network), the DSC peaks became broad and difficult to detect. All the DSC measurements were carried out using the same heating speed of  $5\ ^\circ\text{C}/\text{min}$ ; therefore the extra broadening observed in the case of the gels as compared with pure 8CB is associated with the presence of the network. Therefore we tried to characterize the anisotropic gels

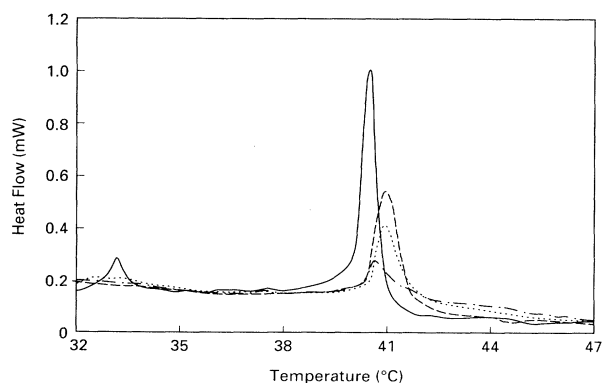


FIG. 1. DSC curves of various gels showing the nematic-to-isotropic transition. —, 100%; — —, 90%; . . ., 80%; - . - . -, 70% 8CB.

and plasticized networks using IR dichroism. The absorbance through samples with an IR beam polarized in the direction parallel ( $A_{\parallel}$ ) and perpendicular ( $A_{\perp}$ ) to the director of the uniaxially oriented system was measured. The dichroic ratio  $R = (A_{\parallel}/A_{\perp})$  and the quantity  $S_o$  are related to the order parameter  $S$  as [8]

$$S_o = \frac{R-1}{R+2} = S(1 - \frac{3}{2} \sin^2\theta), \quad (1)$$

where  $\theta$  is the angle between the direction of molecular orientation and the vibrational transition moment. We used the absorption band at  $2230\ \text{cm}^{-1}$  associated with the  $\text{C}\equiv\text{N}$  stretching vibration in order to estimate  $S_o$  for 8CB and  $S_o$  for C6M molecules was estimated using the  $\text{C}=\text{C}$  benzene ring skeleton vibrations at  $1580\ \text{cm}^{-1}$ . Figure 2 shows  $S_o$  as a function of temperature in a mixture containing 50% w/w C6M before and after polymerization. It can be seen that, within the experimental error, before polymerization  $S_o$  shows the same trend for both 8CB and C6M, i.e., decreasing with increasing temperature before discontinuously becoming zero at  $T_c$  of the mixture showing a typical behavior for nematogens. After polymerization, the behavior of the polymerized C6M (the network) and 8CB molecules becomes different. For the network,  $S_o$  remains almost constant with increasing temperature, while  $S_o$  for 8CB shows a strong decrease up to about  $40\ ^\circ\text{C}$ , above which the decrease becomes more gradual. The behavior shown by the polymerized C6M is explained in terms of the formation of a three-dimensional anisotropic network with chemical cross links. As such a polymeric network is thermally very stable, its order parameter is not expected to show any significant decrease with increasing temperature. The behavior of 8CB within the anisotropic gels and plasticized networks is, however, more complicated and it also differs significantly from the behavior shown by the bulk 8CB, which is also plotted in Fig. 2. In the case of pure 8CB the order parameter becomes zero at the clearing temperature of  $40\ ^\circ\text{C}$ , while in gels and the plasticized

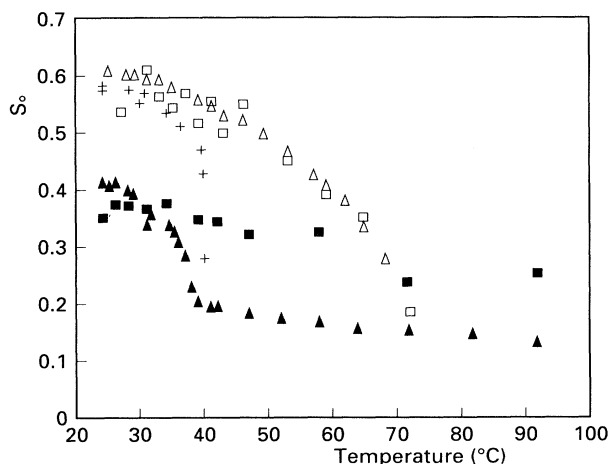


FIG. 2.  $S_o$  as a function of temperature for a mixture containing 50% w/w C6M for C6M (squares) and 8CB (triangles). Open symbols denote before polymerization; solid symbols denote after polymerization at  $71\ ^\circ\text{C}$ . +, pure 8CB in the bulk.

networks the estimated order parameter for 8CB above the clearing temperature is nonzero. This is, in fact, the most important point, showing the difference between the 8CB in the bulk and in the presence of the networks. In order to explain the observed behavior of the 8CB molecules in the presence of an anisotropic network, we should like to invoke a previously suggested two-phase model [1,2]. According to the model, within the gels and anisotropic networks two populations of molecules are present, which are not chemically attached to the network. The behavior of one of the populations (bound fraction) is determined to a large extent by the network and these 8CB molecules do not undergo the first-order nematic-to-isotropic transition, whereas the other population (unbound fraction) behaves much like in the bulk, becoming isotropic at the clearing temperature. However, with IR it is not possible to distinguish these two populations and therefore in order to verify the model we tried to perform control experiments and simulate the results using a theoretical model. According to the two-phase model, the shape of the  $S_o$  curves for 8CB molecules is expected to be dependent on the fraction and the order parameter of the bound molecules within the system. In an attempt to keep the order parameter of the network constant while changing the fraction of the bound molecules, we polymerized various mixtures of C6M and 8CB at room temperature. In Fig. 3(a),  $S_o$  obtained for the network in the gels and plasticized mixtures is plotted as a function of temperature. It can be

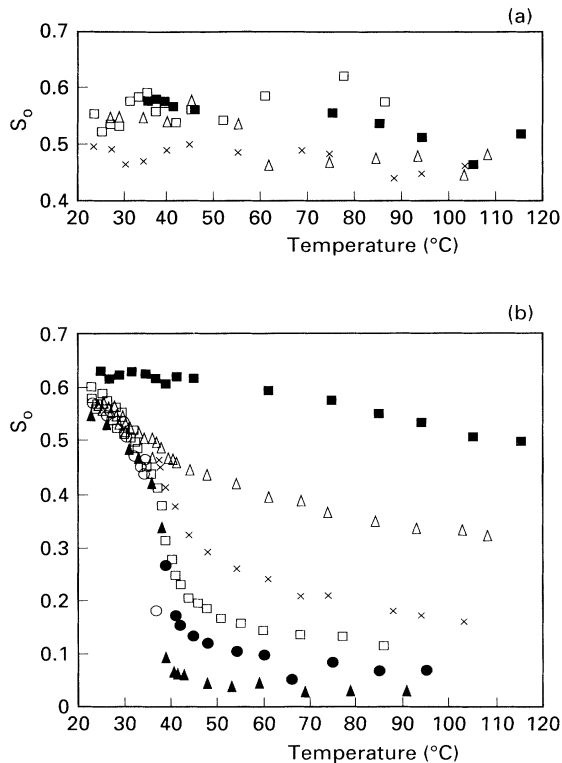


FIG. 3.  $S_o$  as a function of temperature for various mixtures polymerized at 23 °C. ○, 100% 8CB; ▲, 90%; ●, 80%; □, 70%; ×, 60%; △, 40%; ■, 20%. (a) Polymerized C6M. (b) 8CB.

seen that the order parameter of the network within samples of different compositions remains the same and shows only a slight temperature dependence. In the plots of 8CB molecules shown in Fig. 3(b), however, it can be seen that at temperatures below 40 °C the curves tend to merge, whereas at higher temperatures with increasing network concentration the  $S_o$  at a given temperature increases. These results indicate that the bound fraction of 8CB does in fact increase with increasing network fraction within the mixtures. However, the  $S_o$  estimated for 8CB from the IR measurements is an average value containing contributions from both bound and unbound fractions. At temperatures above the clearing temperature of the unbound fraction, the estimated  $S_o$  therefore does not correspond directly to the order parameter of the bound fraction since it also contains a contribution from the isotropic unbound fraction. In order to simulate the effect of the amount of bound fraction and its order parameter on the average  $S_o$  measured using IR, we used the equation below, assuming a two-phase model.

$$R = \frac{A_{\parallel}}{A_{\perp}} = \frac{\epsilon_{\parallel}(b)\phi(b) + \epsilon_{\parallel}(u)\phi(u)}{\epsilon_{\perp}(b)\phi(b) + \epsilon_{\perp}(u)\phi(u)}, \quad (2)$$

where  $\epsilon_{\parallel}$  and  $\epsilon_{\perp}$  are the extinction coefficients in the direction parallel and perpendicular to the director for bound ( $b$ ) and unbound ( $u$ ) fractions ( $\phi$ ), respectively. Temperature dependence of the order parameter of the unbound component was modeled according to the equation below [9]:

$$S_o = \left[ 1 - \frac{T}{T_c} \right]^{0.2}. \quad (3)$$

The order parameter of the bound fraction was assumed to be the same as the order parameter of the network and decreases linearly with increasing temperature. The order parameter of the components was modeled separately and Eqs. (1) and (2) were used to estimate the average  $S_o$  for the two-phase system. In the isotropic state the relation  $\epsilon_{\text{iso}} = (\epsilon_{\parallel} + 2\epsilon_{\perp})/3$  was used. In Fig. 4(a), we have plotted the value of  $S_o$  as calculated for the pure unbound fraction using Eq. (3) and the value of  $S_o$  as calculated for the bound fraction using a linear dependence on temperature, together with the value of  $S_o$  for various mixtures containing various bound and unbound fractions as calculated using Eq. (2). As the bound fraction is strongly related to the network, the order parameter of the bound fraction used in the model can be compared with the order parameter of the network. The trend shown in Fig. 4(a) is very similar to what is observed in Fig. 3(b), where at temperatures below the  $T_c$  (40 °C) curves merge, while at higher temperatures they take the form of parallel lines. Here it is important to point out that the very sharp discontinuous changes at around the  $T_c$  shown by the theoretical curves in Fig. 4(a) are not observed in the case of experimental results. One explanation for this behavior may be the broadening of the nematic-to-isotropic transition of the unbound fraction of 8CB as compared with the behavior shown in the bulk. The validity of this model was further checked by calculating

the effect of keeping the fraction of the unbound molecules constant while varying the order parameter of the bound fraction at a given temperature. In order to obtain anisotropic gels and plasticized networks with bound fractions of various order parameters, mixtures containing 70% w/w [Fig. 5(a)] and 50% w/w [Fig. 5(b)] 8CB were polymerized at various temperatures. In Figs. 5(a) and 5(b) it can be seen that with increasing polymerization temperature the  $S_o$  of the network at a given temperature decreases with increasing polymerization temperature, whereas the  $S_o$  curves obtained for 8CB look very similar and appear to be vertically shifted. Assuming again that the order parameter of the bound fraction of 8CB is determined by the network, these results show the effect of the order parameter and can be compared with the result of the simulations shown in Fig. 4(b). In the simulations the bound fraction was kept at 60% and the order parameter of the bound fraction was varied. In Fig. 4(b) the order parameter of the bound fraction (corresponding also to the order parameter of the network) is plotted together with the average  $S_o$  for composite systems as a function of temperature. It can be seen that, just as in the experimental case (Fig. 5), the curves appear

to be vertically shifted. These results provide further support to the two-phase model suggested to explain the behavior of the molecules which are not chemically attached to the network.

Based on the two-phase model, we also tried to estimate the fractions of bound and unbound 8CB molecules in various systems. For this purpose we used the  $S_o$  curves obtained for 8CB molecules in Fig. 3(b) together with the  $S_o$  estimated for the network [Fig. 3(a)], which was taken to represent the order parameter of the bound fraction of 8CB. Above the nematic-to-isotropic transition temperature Eq. (2) reduces to a simple form; therefore, to calculating the bound and unbound fractions, we used the values of  $S_o$  measured at 50 °C in Fig. 3. Figure 6 shows the estimated bound fractions of 8CB in anisotropic gels and plasticized networks and as expected the fraction of the bound 8CB molecules increases with increasing network fraction.

Having simulated the behavior of the 8CB molecules using the two-phase model, we tried to monitor the changes occurring during the polymerization of the C6M molecules (the formation of the network) leading to the formation of bound and unbound fractions of 8CB within

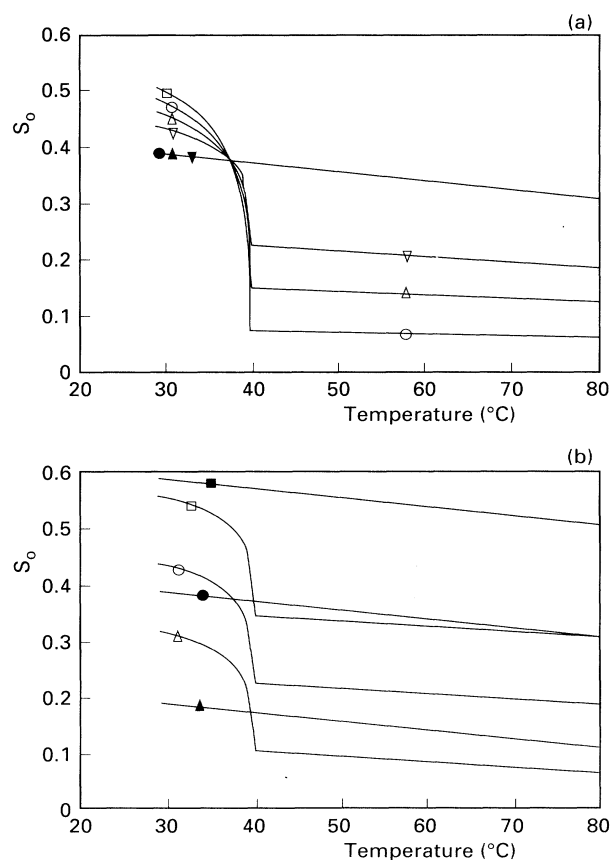


FIG. 4. Simulated  $S_o$  as a function of temperature for bound fractions (solid symbols) and average for both bound and unbound fractions (open symbols). (a) Systems with various bound fractions:  $\square$ , 0%;  $\circ$ , 20%;  $\triangle$ , 40%;  $\nabla$ , 60% w/w. (b) System containing a bound fraction of 60% w/w with various-order parameters.

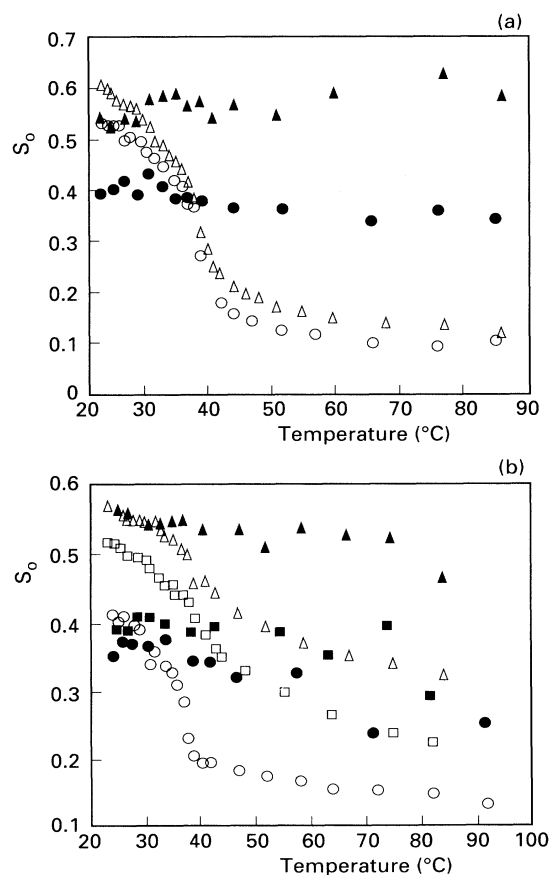


FIG. 5.  $S_o$  as a function of temperature for 8CB (open symbols) and C6M (solid symbols) after polymerization at  $\triangle$ , 23 °C;  $\square$ , 44 °C;  $\circ$ , 71 °C for mixtures containing (a) 70% w/w 8CB and (b) 50% w/w 8CB.

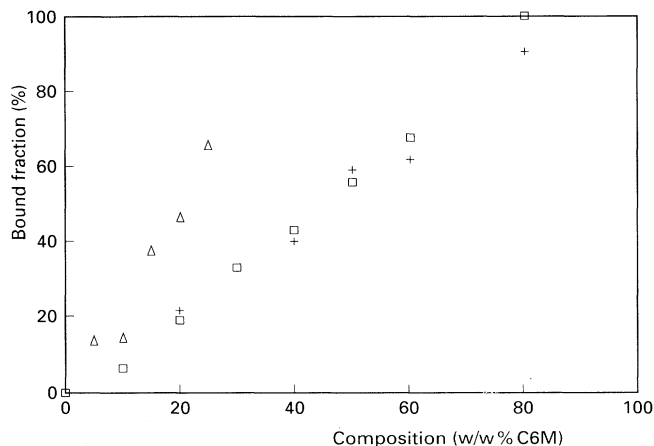


FIG. 6. Bound fractions of 8CB in anisotropic gels and plasticized networks containing various amounts of C6M estimated using +, IR; □, retardation; △, DSC.

these mixtures. The mixtures were filled into cells where uniaxial orientation of the molecules was induced by the orientation layers. The cells were placed between crossed polarizers and the transmission of monochromatic light (546 nm) was monitored as a function of time as the samples were irradiated with 366 nm ( $0.5 \text{ mW cm}^{-2}$ ) from a high-pressure mercury source. In Fig. 7, the change in retardation is shown as a function of time for various mixtures polymerized just above the clearing temperature of 8CB. It can be seen that, after a short induction time, the retardation decreases continuously before reaching a constant level as a result of polymerization. We would like to describe this behavior also in terms of the two-phase model. It has already been shown that two distinct populations of 8CB are present within these systems. This indicates that, during polymerization, the system probably phase separates into polymer-rich and polymer-poor regions as a result of network formation. Within these regions, as the polymerization proceeds fur-

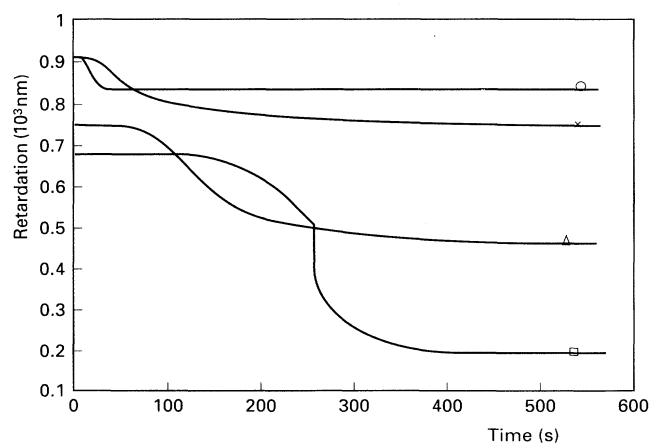


FIG. 7. Retardation as a function of time during the polymerization of systems containing various amounts of C6M. □, 10%; △, 30%; ×, 50%; ○, 80% w/w.

ther, C6M becomes attached to the network and the system becomes depleted of monomeric C6M. In the polymer-poor regions, as monomeric C6M reacts and gets out of the monomeric mixture, the clearing temperature of the mixture in these domains decreases, eventually causing these regions to become isotropic since the polymerization is carried out above the  $T_c$  of 8CB. Indeed, this effect can be seen in Fig. 7 most clearly for the sample containing 10% C6M where the decrease in retardation during polymerization becomes discontinuous. Thus after the phase separation, during further polymerization,  $T_c$  in the polymer-poor phase becomes lower. As given in Eq. (3), the reduced temperature ( $T/T_c$ ) is what determines the order parameter; therefore as a result of a decrease of  $T_c$  in the polymer-poor regions the order parameter and thus the birefringence decreases. In the case of the polymer-rich regions, however, the behavior of 8CB is probably determined to a large extent by the network and the order parameter and the birefringence in these regions remain slightly affected as a result of further polymerization. Here we would like to associate the previously defined bound fraction of 8CB with the molecules in the polymer-rich regions and the unbound fraction with the molecules in polymer-poor regions. The fact that the bound fraction increases with increasing network concentration (see Fig. 6) supports the suggestion that the bound fraction of 8CB is associated with the polymer-rich regions, since with increasing C6M concentration in a phase-separated system the polymer-rich regions are also expected to increase. We therefore also tried to estimate different fractions of 8CB using the results from the retardation experiments. In Fig. 7 it can be seen that in all cases after an initial decrease the retardation eventually reaches a constant level and shows no further decrease with increasing time and the decrease in the retardation increases with increasing 8CB concentration. As the decrease in the retardation during polymerization is assumed to be caused partly by the unbound fraction of the 8CB molecules becoming isotropic and partly by the C6M molecules decreasing their degree of order during polymerization, we used the values for the decrease in retardation in order to calculate the unbound fraction of 8CB which becomes isotropic during polymerization; the results are shown in Fig. 6. It can be seen that the results conform well with the values obtained using the IR measurements. Here it is also interesting to compare the bound fraction estimated using DSC based on the exothermic peaks associated with the nematic-to-isotropic transition of 8CB. The procedure involved in the estimation of the bound fraction using DSC is explained in more detail in Ref. [1]. It involves estimating the transition enthalpy for the nematic-to-isotropic transition in gels and plasticized networks by only taking nonreactive molecules within the system into account. The transition enthalpy decreases with increasing network fraction and the percentage decrease is associated directly with the bound fraction. It can be seen that the values obtained using DSC for the bound fraction are larger than the values estimated using IR and birefringence measurements. In DSC calculations, as the peaks became broader with increasing network concen-

tration, the estimation became difficult. This effect of the broadening of the isotropic transition temperature is also manifested in IR curves, where the large decrease in the  $S_0$  for 8CB close to  $T_c$  occurs also over a broad temperature range. Therefore the use of DSC probably results in an overestimation of the bound fraction.

In order to study the structure within the anisotropic gels, x-ray diffraction was used. Here we used mainly the small-angle peaks to get an insight into the packing behavior of the 8CB molecules. The smectic-to-nematic transition within these systems falls beyond the scope of the present work and it will not be discussed in this article. There are a number of publications [10,11] describing x-ray-diffraction work on 8CB. In these publications the nematic-to-smectic- $A$  transition within the system is also described. It has been shown that the correlation lengths along ( $\xi_{\parallel}$ ) and perpendicular to ( $\xi_{\perp}$ ) the director in the smectic- $A$  phase are the same. As the system becomes nematic, the correlation lengths start to diverge,  $\xi_{\perp}$  becoming smaller than  $\xi_{\parallel}$ . In Fig. 8 x-ray-diffraction patterns obtained for pure 8CB in the smectic- $A$  and isotropic phases are shown together with the patterns obtained for polymerized samples containing 70% and 50% w/w

8CB. In all cases the small-angle peaks correspond to a periodicity of 3.2 nm within samples associated with the smectic bilayer spacing of 8CB. No peaks corresponding to the C6M molecules with an end-to-end distance of about 4.2 nm were present. In the case of pure 8CB it can be seen that in the smectic phase the small-angle peaks are round, conforming well with the literature reports that  $\xi_{\parallel}$  and  $\xi_{\perp}$  are the same. X-ray-diffraction pictures obtained for gels and plasticized networks, however, are quite different. These differences can be summed up as follows. For these samples at room temperature the small-angle peaks appear to be broader in the direction perpendicular to the director, indicating that the  $\xi_{\parallel}$  is larger than  $\xi_{\perp}$ . For pure 8CB at the same temperature,  $\xi_{\parallel}$  and  $\xi_{\perp}$  are the same. Furthermore, at room temperature the samples show sharp small-angle diffraction peaks superimposed on broader peaks which appear in the background; this is clearest in the case of the sample containing 50% network. At 50 °C, which is above the nematic-to-isotropic transition temperature of 8CB, the sharp peaks exhibited by the gels and plasticized networks disappear, leaving behind only the broad background. Furthermore, as opposed to the pure 8CB, in ad-

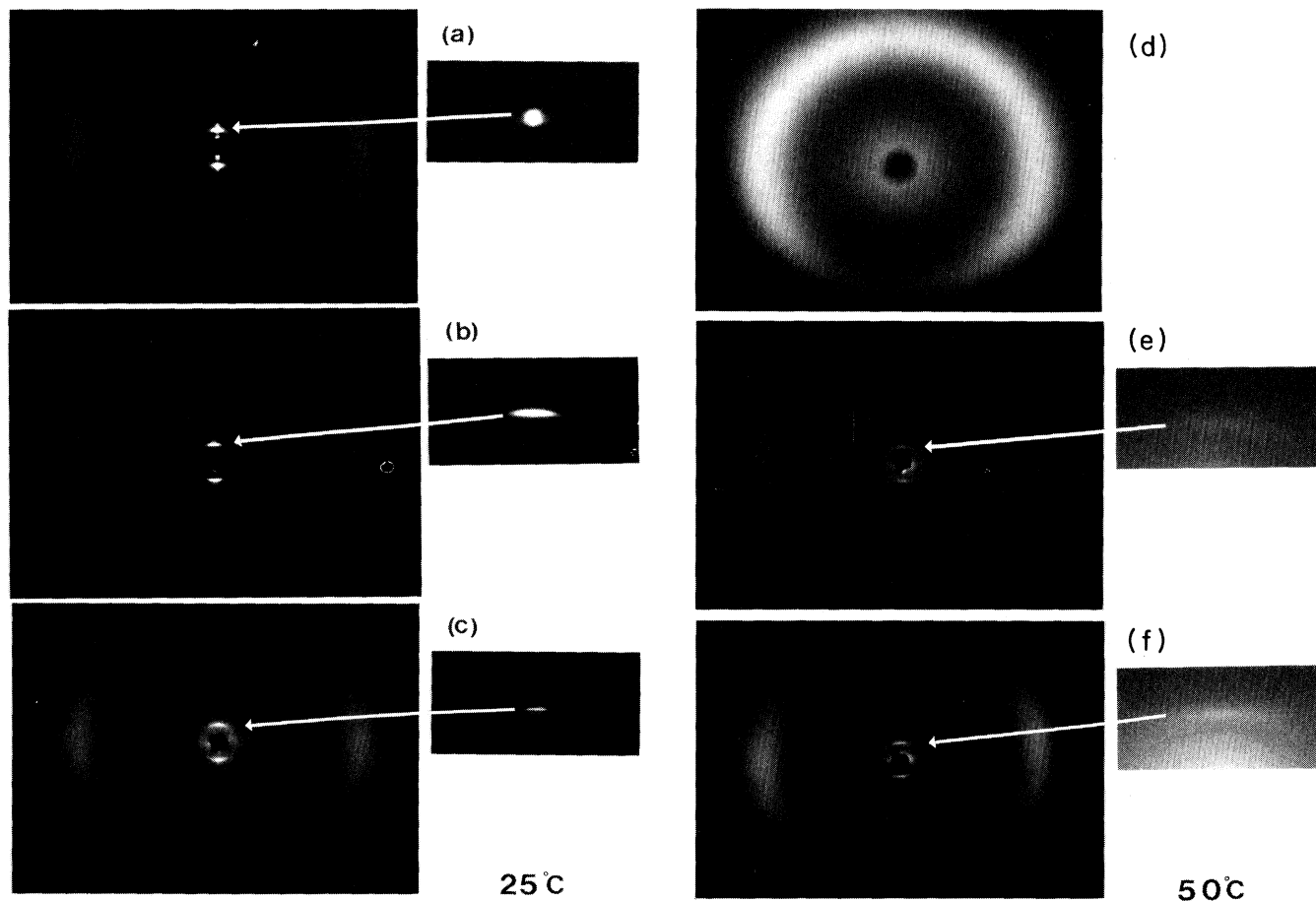


FIG. 8. X-ray-diffraction photographs for pure 8CB and polymerized systems containing various amounts of C6M at various temperatures. (a) Pure 8CB at 25 °C, (b) 70% 8CB at 25 °C, (c) 50% 8CB at 25 °C, (d) pure 8CB at 50 °C, (e) 70% 8CB at 50 °C, and (f) 50% 8CB at 50 °C.

dition to the first-order small-angle peaks, second-order and even third-order peaks are also observable for the broad peaks. The sharp peaks, however, do not show higher orders. In a simple model the intensity of the  $n$ th order of reflection will be proportional to [12]  $\exp(-4\pi^2 n^2 \langle z^2 \rangle / d^2)$ , where  $(\langle z^2 \rangle)^{0.5}$  is the average longitudinal displacement of the molecule caused by thermal fluctuations. We would like to associate the diffraction peaks shown in Fig. 8 with bound and unbound molecules within the gels and plasticized networks. The sharp peaks which do not show higher orders and disappear above the clearing temperature of 8CB are more likely to be caused by the unbound fraction of 8CB molecules. They also do not show higher orders as is the case with pure 8CB, indicating that the layer thickness is not regular as a result of thermal fluctuations. The broad peaks, however, are more likely to be caused by the bound fraction as they do not disappear even above the isotropic transition temperature of 8CB and show higher orders. The fact that the broad peaks show higher orders indicates that the bound molecules are influenced to a lesser extent by thermal fluctuations. As mentioned before, the breadth of the small-angle peaks in the case of samples containing 70% and 50% C6M in different directions is different. Using the sharp peaks observed for the sample containing 50% 8CB at 25 °C, the correlation lengths in different directions were estimated to be  $\xi_{\parallel} = 300$  nm and  $\xi_{\perp} = 25$  nm from  $\xi = \lambda / \Delta\theta$ , where  $\Delta\theta$  is the angular width of the scattering curve measured in different directions at half-height. No curve fitting was attempted since these sharp peaks were already superimposed on broad peaks and on correction for the nonlinear darkening of the x-ray film. For 8CB molecules in porous silica it has already been shown [13] that the  $\xi_{\parallel}$  and  $\xi_{\perp}$  are limited by the pore size of the silica. Here the fact that correlation length in various directions is different indicates that within the gels and plasticized networks  $\xi_{\parallel}$  and  $\xi_{\perp}$  are limited by the network. Based on the x-ray-diffraction results, we would like to suggest the schematic representation shown in Fig. 9 in order to describe the structure of the network within the gels and plasticized networks. In this schematic representation domains in the form of channels are formed by the network molecules confining 8CB and limit the correlation lengths. The other reason for suggesting such a thin-layered structure is twofold. First, scanning-electron-microscopic studies of the freeze-fractured surfaces did not show Swiss cheese or a bushy structure observed for isotropic networks obtained by the polymerization of isotropic diacrylates [14] in mixtures of nonreactive LC molecules characterizing binodal and spinodal decompositions. Furthermore, the absence of small-angle peaks corresponding to polymerized C6M molecules showed the absence of long-range correlation between the center of gravity of the molecules. This is probably due to the absence of bulky blocks of polymerized C6M in the anisotropic gels and plasticized networks since in the bulk polymerized C6M small-angle diffraction peaks are observed. Second, the observed high-order parameters for the network molecules within the anisotropic gels and plasticized networks require a particular type of packing

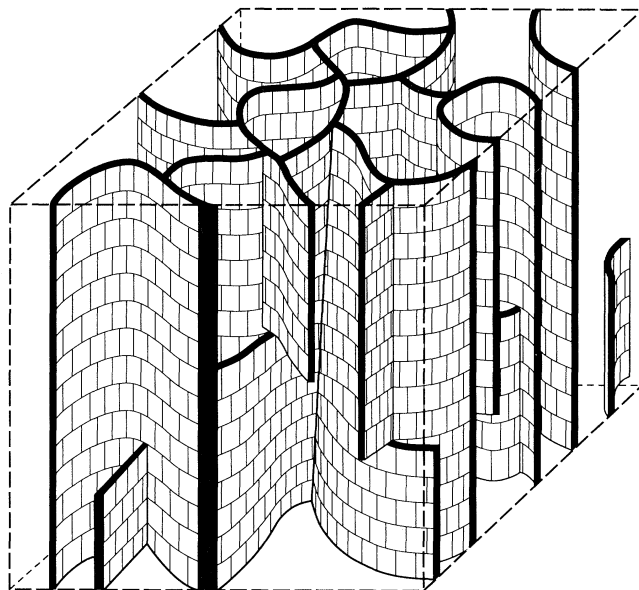


FIG. 9. Schematic representation of a gel structure.

and such a packing is likely to lead to the structure shown in Fig. 9. The argument is as follows. Upon polymerization of C6M acrylate main chains (represented by lines running perpendicular to the director in Fig. 9) connected to each other, the mesogenic units (represented by the short lines in Fig. 8) are formed. Every other carbon atom along the acrylate main chain has a mesogenic unit attached to it sideways. Thus the distance between the points where the molecules are attached to the same backbone is about 0.25 nm. However, the nearest-neighbor distance between the mesogenic groups estimated from the wide-angle peaks is on the order of 0.5 nm. In the closest packing state 0.5 nm corresponds to the minimum distance between the benzene rings of the mesogenic group. For C6M molecules to have the mean neighbor distance of 0.5 nm in the bulk and 0.25 nm along the main chain without causing a drastic decrease in the degree of orientational order, it is necessary that to a large extent adjacent mesogenic units along the main chain are oriented in opposite directions. Therefore, in such a sterically hindered structure, during polymerization growth of the polymer is likely to be confined to planes, giving rise to the structure schematically represented in Fig. 9.

## CONCLUSIONS

It has been shown that anisotropic networks containing LC molecules which are not chemically attached to the network can be made. The behavior of the LC molecules in the presence of the anisotropic network was found to be very different to that in the bulk. In order to explain the behavior of the molecules which are not chemically attached to the network (8CB) as observed by IR dichroism a two-phase model was suggested. The model, which assumes two populations of 8CB molecules [(i) 8CB molecules bound by the network, showing no

first-order nematic-to-isotropic phase transition and (ii) unbound 8CB molecules behaving as in the bulk], was used in simulations which conformed well with the experimentally observed behavior. Based on the optical retardation measurements, the most likely cause of the existence of the two populations of 8CB was the phase separation induced during the formation of the network (polymerization of C6M), resulting in polymer-poor and polymer-rich regions. Using x-ray diffraction, it was shown that within the anisotropic gels and plasticized networks the 8CB molecules are contained in channels formed by the network. However, the question of the

critical domain dimensions below which the first-order nematic-to-isotropic phase transition is suppressed still remains an open question as there is no direct way of measuring the domain size within these systems.

#### ACKNOWLEDGMENT

We would like to thank Dr. H. Boots for many useful discussions during this work.

- 
- [1] R. A. M. Hikmet, *Liq. Cryst.* **9**, 405 (1991).  
[2] R. A. M. Hikmet and B. H. Zwerver, *Liq. Cryst.* **10**, 835 (1991).  
[3] R. A. M. Hikmet and B. H. Zwerver, *Liq. Cryst.* **12**, 319 (1992).  
[4] R. A. M. Hikmet and C. de Witz, *J. Appl. Phys.* **70**, 1265 (1991).  
[5] R. A. M. Hikmet, *Mol. Cryst. Liq. Cryst.* **213**, 117 (1992).  
[6] R. A. M. Hikmet and B. H. Zwerver, *Liq. Cryst.* **13**, 561 (1993).  
[7] D. J. Broer, R. A. M. Hikmet, and G. Challa, *Makromol. Chem.* **190**, 2255 (1990).  
[8] R. Kiefer and G. Baur, *Mol. Cryst. Liq. Cryst.* **174**, 101 (1989).  
[9] W. H. De Jeu, *Physical Properties of Liquid Crystalline Molecules* (Gordon and Breach, New York, 1980).  
[10] D. Davidov, C. R. Safinya, M. Kaplan, S. S. Dana, R. Schaetzing, R. J. Birgeneau, and J. D. Lister, *Phys. Rev. B* **19**, 1657 (1979).  
[11] A. J. Leadbetter, J. C. Frost, J. P. Gaughan, G. W. Gray, and A. Mosley, *J. Phys. (Paris)* **40**, 375 (1979).  
[12] P. Davidson and A. M. Levelut, *Liq. Cryst.* **11**, 469 (1992).  
[13] T. Bellini, N. A. Clark, C. D. Muzny, D. A. Chris, L. Wu, C. W. Garland, D. W. Schaefer, and B. J. Oliver, *Phys. Rev. Lett.* **69**, 788 (1992).  
[14] J. W. Doane, A. Golemme, J. L. West, J. B. Whitehead, and B. G. Wu, *Mol. Cryst. Liq. Cryst.* **165**, 511 (1988).



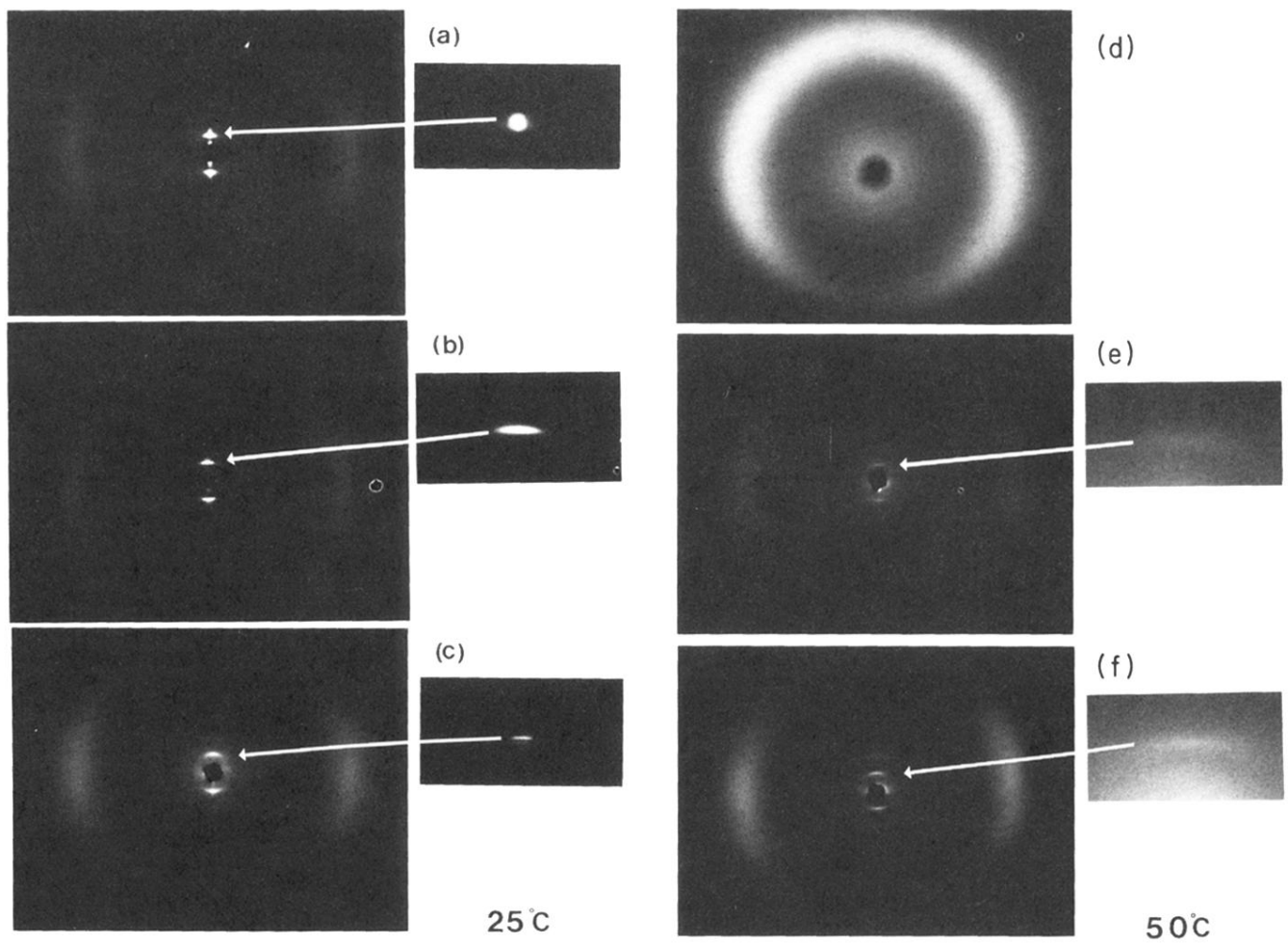


FIG. 8. X-ray-diffraction photographs for pure 8CB and polymerized systems containing various amounts of C6M at various temperatures. (a) Pure 8CB at 25 °C, (b) 70% 8CB at 25 °C, (c) 50% 8CB at 25 °C, (d) pure 8CB at 50 °C, (e) 70% 8CB at 50 °C, and (f) 50% 8CB at 50 °C.